Surface & Coatings Technology 228 (2013) S190–S193

Contents lists available at SciVerse ScienceDirect

Surface & Coatings Technology

journal homepage: www.elsevier.com/locate/surfcoat

Stress reduction of diamond-like carbon by Si incorporation: A molecular dynamics study

Xiao-Wei Li [a,b], Min-Woong Joe [b], Ai-Ying Wang [a,*], Kwang-Ryeol Lee [b,*]

[a] Division of Surface Engineering, Ningbo Institute of Material Technology and Engineering, Chinese Academy of Sciences, Ningbo 315201, PR China
[b] Computational Science Research Center, Korea Institute of Science and Technology, Seoul 136-791, South Korea

ARTICLE INFO

Available online 16 June 2012

Keywords:
Diamond-like carbon
Residual stress
Si incorporation
Molecular dynamics simulation

ABSTRACT

The residual stress and atomic bond structure of Si-incorporated diamond-like carbon films were investigated by the molecular dynamics simulation using Tersoff interatomic potential. The effect of Si incorporation into amorphous carbon matrix was analyzed for the various Si concentrations ranging from 0 to 2.1 at.%. The present simulation revealed that the incorporation of a small amount of Si significantly reduced the residual compressive stress: when the Si content was 0.54 at.%, the minimal compressive stress of 1.4 GPa was observed. Structural analysis using the radial distribution function and the bond angle distribution indicated that the compressive stress reduction resulted from the relaxation of highly distorted bond angles less than 109.5°.

1. Introduction

Owing to its high hardness, low friction coefficient and chemical stability [1,2], diamond-like carbon (DLC) films are not only widely used as a mechanical protective coating in various industrial applications, but also considered as a strong candidate for medical applications, such as heart valves [3,4], vascular stent [5] and artificial joint [6]. However, high level of residual compressive stress that is closely related with the distorted atomic bonds in amorphous carbon structure deteriorates the adhesion between the film and the substrate, leading to the failure of the coated surface.

Many efforts have been thus made to decrease the stress of DLC films by controlling the substrate bias during deposition [7], multilayer nanostructure coating [8], third element doping [9] and adapting post-annealing process [10]. Third element doping has aroused more research interest because the third element incorporation can improve tribological or biological performance of the coating in addition to the reduction of the residual stress [11–14]. For example, a significant decrease in the residual compressive stress of tetrahedral amorphous carbon films was observed when a small amount of Si was incorporated [11]. It was also reported that the tribological properties and anti-corrosion properties were also improved by Si incorporation [15,16]. However, the effect of third element addition on the atomic bond structure is yet to be clarified, because of the limited experimental characterization of the atomic bond structure.

Computational simulation technique in atomic scale provides a robust method for deeper insight of the atomic bond structure and the properties of a diamond-like carbon film. In diamond-like carbon films, the thermal spike and sub-plantation models for the sp^3 hybrid bond formation have been intensively tested by the atomic scale simulation [17–19], whereas Marks et al. [20] proposed a new model of energetic burial. Many simulation studies reproduced the structure and property variations with kinetic energy of deposited carbon atoms, which led to understand the growth process in atomic scale [21–23].

Most of the previous computational results focused on the mechanism of sp^3 bond formation and the dependence of the atomic bond structure on the kinetic energy of the deposited species in pure carbon or hydrocarbon system. In contrast, computational study on the third element addition during diamond-like carbon growth is highly limited. In the present work, we performed a classical MD simulation to investigate the structure and the residual stress of Si-incorporated DLC films using Tersoff interatomic potential for Si–C system. Structural analysis of the film in atomic scale revealed that the Si atom is very effective to relax the bond angle distortions, which results in the significant stress reduction.

2. Computational method

In order to simulate the deposition and structure of Si-incorporated DLC films, Tersofff potential for the Si–C system was used. Tersoff potential, which is a three body empirical potential considering dependence of bond order on the local environment, was firstly introduced for pure Si and has been successfully applied to various Si systems [24,25]. Tersoff also suggested an empirical potential for carbon or multicomponent system with the identical form to that for Si, but with different numerical values of the parameters [26,27]. Even if the calculated results have revealed the limit of the potential that π bonding is not

* Corresponding authors.
E-mail addresses: aywang@nimte.ac.cn (A.-Y. Wang), krlee@kist.re.kr (K.-R. Lee).

0257-8972/$ – see front matter © 2012 Elsevier B.V. All rights reserved.
doi:10.1016/j.surfcoat.2012.06.031

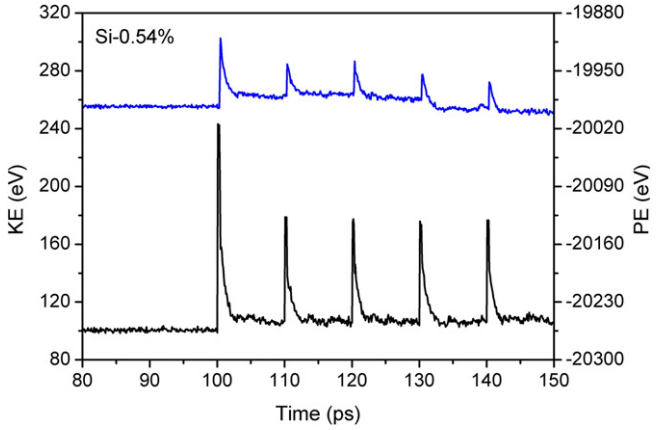

Fig. 1. Energy change during deposition process of the first five incident C atoms. In this figure, the upper blue one corresponds to the PE curve, the other is the KE curve.

adequately considered [28–30], the Tersoff potential is still an effective potential for simulating the C–Si system.

Energetic atoms of C and Si impacted on a diamond (001) single crystal substrate of $7a_0 \times 7a_0 \times 6.75a_0$, where a_0 is the equilibrium lattice constant of bulk diamond. The diamond substrate was composed of 2800 carbon atoms with 100 atoms per layer and was equilibrated at 300 K for 100 ps before deposition. The incident atoms were deposited at the position of 10 nm above the substrate surface at a random {x, y} position. While the positions of atoms in the bottom two layers were frozen to mimic the bulk substrate, all the other atoms were unconstrained. The incident kinetic energy of incident C or Si atoms was fixed at 70 eV/atom because the optimum energy for a highly stressed and dense a-C film deposition is known to be in the range from 50 to 100 eV/atom [28,29]. 5000 carbon atom deposition was simulated and the concentration of Si was varied from 0 at.% to 2.1 at.%. The periodic boundary conditions were applied in x and y directions, and the time step for simulation was fixed at 1 fs.

The time interval between two consecutive C atoms depositing on the substrate was fixed at 10 ps, which corresponded to an impracticable ion flux of $1.57 \times 10^{27}/m^2$ s. Fig. 1 shows the changes in potential and kinetic energy of the system during deposition of the first five incident C atoms. The peaks in Fig. 1 were explained in a previous publication [29]. The energy change in the system shows that most of the substantial reaction occurred during 2 or 3 ps after an energetic carbon bombardment. The time interval of 10 ps was thus enough for relaxing the atomic structure and diminishing the unrealistic effect of high carbon flux on the deposition process. The temperature of the substrate was rescaled to 300 K after the atomic rearrangement caused by the bombardment of incident atom was finished. It can be thus said that the present simulation reasonably mimics the real deposition behavior even if the simulation itself was under an accelerated condition.

3. Results and discussion

Fig. 2 shows the final morphologies for pure DLC and Si-incorporated DLC films. Green spheres represent the deposited carbon atoms while blue ones are the substrate carbon atoms. Si atoms are presented by red spheres. All the deposited films are amorphous as will be described later by the radial distribution function (RDF). The incorporation of a small amount of Si atoms has little effect on the film thickness; the film thickness is about 5.9 nm for all the cases of Si concentration.

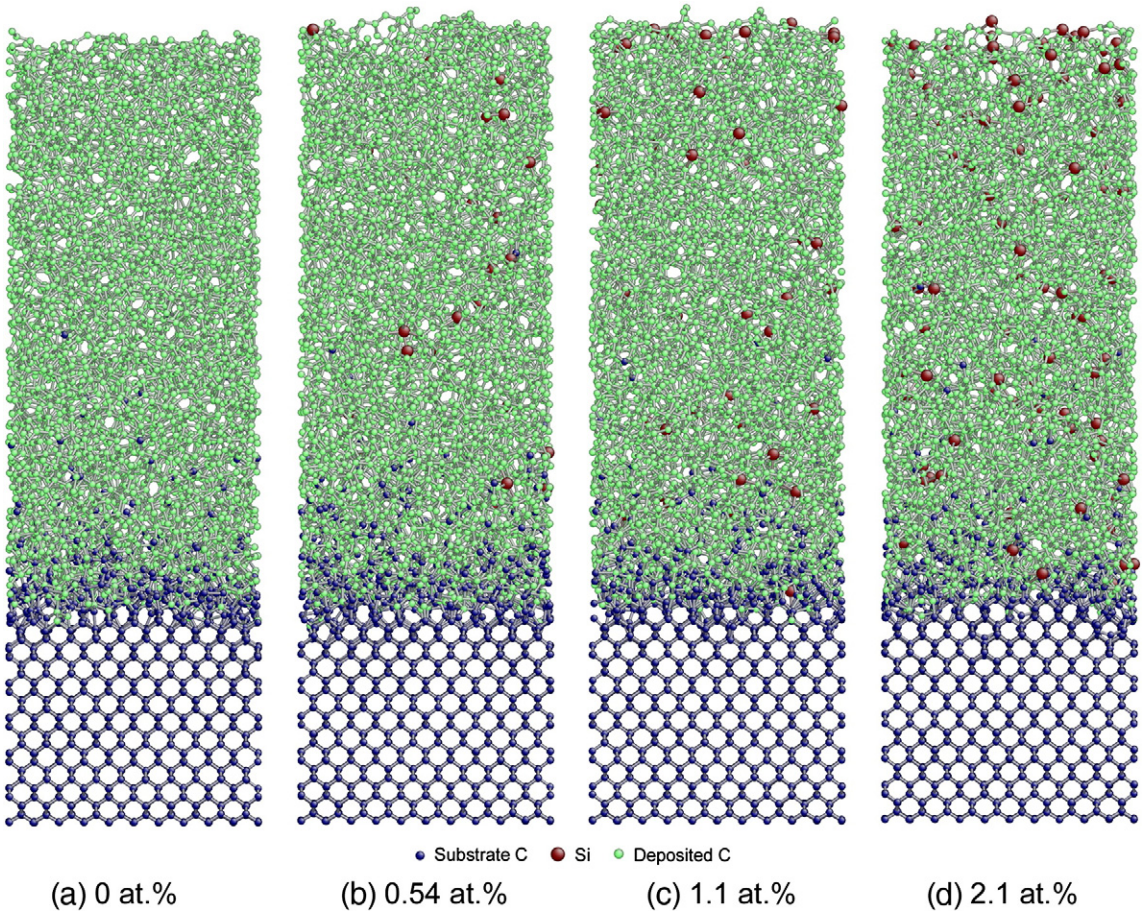

Fig. 2. The snapshots of DLC films with various Si concentrations.

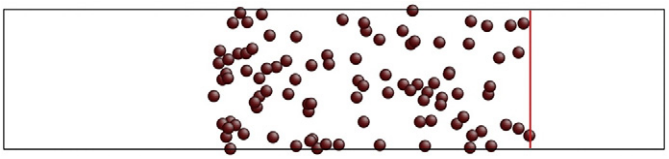

Fig. 3. Si distribution in DLC films when Si concentration is 2.1 at.%.

Since the kinetic energy of the incident atoms is much higher than the cohesive energy of diamond (7.6–7.7 eV/atom), the incident atoms penetrated into the diamond lattice and intermixed with the substrate atoms. Significant intermixing layer between the film and the substrate was observed in Fig. 2. Incorporated Si atoms are uniformly distributed throughout the films, as illustrated in Fig. 3.

Before characterizing the film properties such as density and sp^3 fraction, variation of the properties with depth was investigated. Fig. 4 shows the variations of number density and hybridization ratio along the film growth direction when the Si concentration was 0.54 at.%. It reveals that the whole system is divided into four regions including substrate, transition region, steady state growth region and surface region. Because of the intermixing on the substrate surface, structural gradient exits at the interface leading to the change in the physical properties. The surface region is also markedly relaxed. Therefore, the physical quantities of the film were quantified in the steady state growth region of thickness of 3.5 nm (gray region of Fig. 4), where the number density and hybridization ratio exhibited a relatively constant value. One should note that the sp^3 fraction in all films appears low with values around 10 to 20%. It might attribute to the limit of Tersoff potential that the formalism was originally developed for Si system where no π bonding needs to be exactly described.

Fig. 5 shows the dependence of the calculated residual stress and the number density on the Si concentration. Pure DLC film had a high residual compressive stress, larger than 15 GPa. However, the incorporation of 0.54 at.% of Si significantly reduced the compressive stress down to 1.4 GPa. Further incorporation of Si slightly increased the residual stress. The significant reduction in the residual stress of tetrahedral amorphous carbon by the small amount of Si incorporation was consistent with the previous experimental results [11]. The number density changed in a similar manner to that of the residual stress. With the Si incorporation, number density decreased to 0.215 mol/cm^3 from 0.251 mol/cm^3 of pure DLC film. However, it must be noted that the variation in the number density (max. 14%) is much smaller than the residual stress reduction (max. 90%).

In order to elucidate the properties in terms of the atomic bond structure variation, the radial distribution function and bond angle distribution were analyzed. The radial distribution functions (RDF)

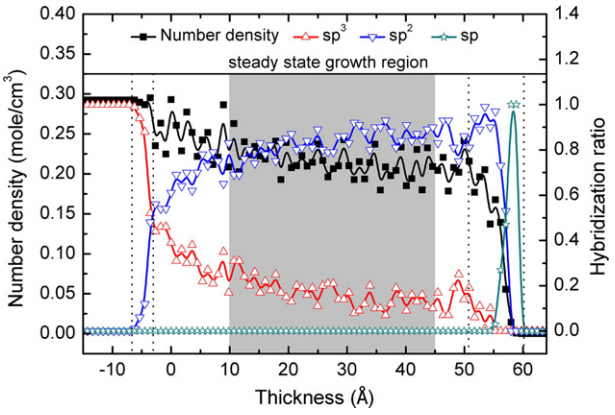

Fig. 4. Variations of number density and hybridization ratio along the growth direction under Si concentration of 0.54 at.%. The positive direction corresponds to the films, while the negative direction corresponds to the original substrate.

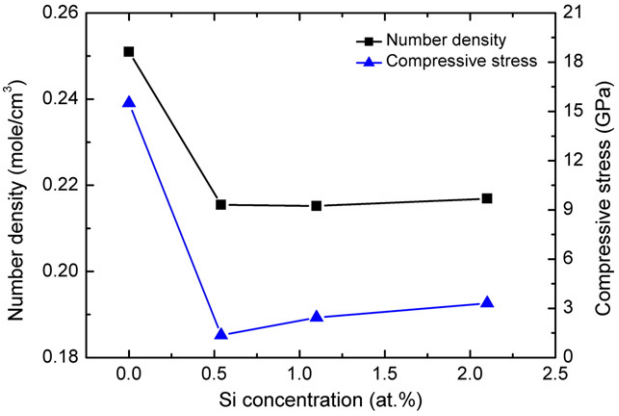

Fig. 5. Variations of the residual compressive stress and number density with Si concentration in Si-incorporated DLC films.

of the Si-incorporated DLC films are illustrated in Fig. 6. For comparison, the RDF of pure DLC film was also included. First of all, the RDF spectra show that all the films are amorphous without exhibiting a long range order. The red broken vertical lines represent the first nearest neighbor (1.54 Å) and the second nearest neighbor distance (2.52 Å) of crystalline diamond. The first nearest neighbor distances for Si–C and Si–Si are 1.94 Å (blue broken vertical line) and 2.34 Å (green broken vertical line), respectively. For pure DLC film, the 2nd C–C nearest neighbor peak is located at 2.53 Å which is similar to that of diamond. On the other hand, the first nearest neighbor peak for C–C (1. 48 Å) is much smaller than that of diamond. The decrease in the C–C bond distance would be the major reason for the high compressive stress of DLC film. With Si incorporation, the positions of the 1st nearest neighbor peaks have almost no shift comparing with those of pure DLC film. Therefore, it can be said that the incorporated Si atoms have little effect on the bond distance of DLC film. However, it would be noted that the shape of the 2nd nearest neighbor peak changed with the Si incorporation, even if one considers the small shoulder at the position of 2.1 Å as the "false peak" caused by the cut-off radius of the potential function [20,30]. Because the 2nd nearest peak is dependent on both bond angle and bond distance, these results implied that a significant bond angle change occurred by the Si incorporation.

More direct evidence of the bond angle change was revealed by the bond angle distribution analysis. Fig. 7 shows the bond angle distribution of pure DLC film and the Si-incorporated DLC films. The equilibrium bond angle of graphite is 120° and that of diamond is 109.5°. In pure DLC film, large population of the bond angle below

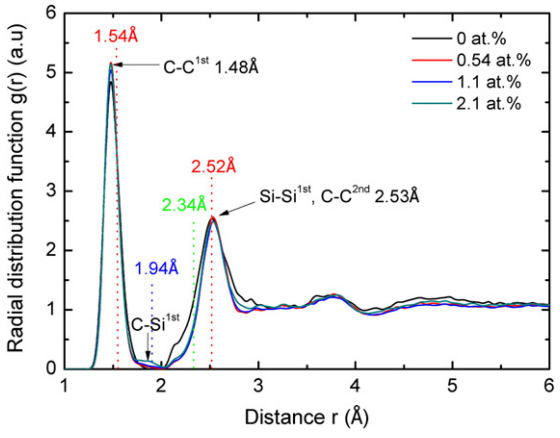

Fig. 6. Radial distribution functions of pure DLC and Si-incorporated DLC films.

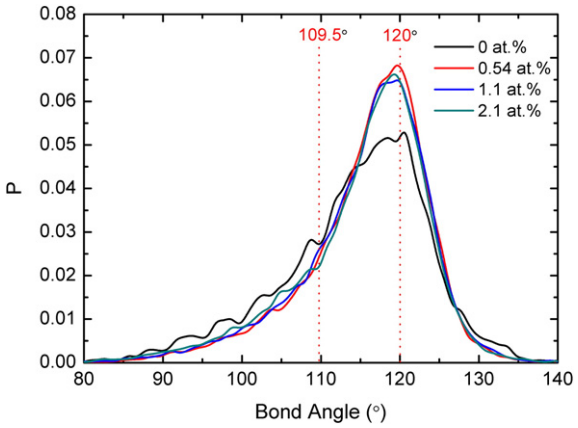

Fig. 7. Bond angle distribution functions of pure DLC and Si-incorporated DLC films.

109.5° was observed. In addition to the reduced bond distance (Fig. 6), the bond angle distortion would also contribute to the high compressive stress. Small amount of Si incorporation (see red curve in Fig. 7 for 0.54 at.% incorporation) considerably reduces the population of the bond angle smaller than 109.5°, whereas the population of bond angle near 120° increases with Si incorporation. These results suggest that the incorporation of Si atoms resulted in the relaxation of distorted bond and the reduction in the residual compressive stress.

4. Conclusion

Molecular dynamics simulation of the Si incorporated DLC film reproduced the experimental observation that the residual stress significantly decreased with a little degradation of the atomic number density of the film with Si incorporation [11]. By the analysis of radial distribution function and bond angle distribution, it was revealed that the Si incorporation efficiently relaxed the distorted bonds in the amorphous carbon matrix, resulting in the reduction of the residual compressive stress.

Acknowledgments

The present research was supported by the projects of the National Natural Science Foundation of China (Grant No. 51072205) and the Natural Science Foundation of Zhejiang Province (Grant No. Y4100312). Works at Korea Institute of Science and Technology was financially supported by the Core Capability Enhancement Program (2E22200) and a grant (2010K000298) from 'Center for Nanostructure Materials Technology' under '21st Century Frontier R&D Programs' of the Ministry of Science and Technology, Korea.

References

[1] J. Brand, R. Gadow, A. Killinger, Surf. Coat. Technol. 180–181 (2004) 213.
[2] A.H. Lettington, Carbon 36 (1998) 555.
[3] R. Hauert, Diamond Relat. Mater. 12 (2003) 583.
[4] N. Ali, Y. Kousar, T.I. Okpalugo, V. Singh, M. Pease, A.A. Ogwu, J. Gracio, E. Titus, E.I. Meletis, M.J. Jackson, Thin Solid Films 515 (2006) 59.
[5] P.D. Maguire, J.A. McLaughlin, T.I.T. Okpalugo, P. Lemoine, P. Papakonstantinou, E.T. McAdams, M. Needham, A.A. Ogwu, M. Ball, G.A. Abbas, Diamond Relat. Mater. 14 (2005) 1277.
[6] A.S. Loir, F. Garrelie, C. Donnet, J.L. Subtil, M. Belin, B. Forest, F. Rogemond, P. Laporte, Appl. Surf. Sci. 247 (2005) 225.
[7] D. Sheeja, B.K. Tay, S.P. Lau, X. Shi, Wear 249 (2001) 433.
[8] C. Mathioudakis, P.C. Kelires, Y. Panagiotatos, P. Patsalas, C. Charitidis, S. Logothetidis, Phys. Rev. B 65 (2002) 205203-1.
[9] M. Ban, T. Hasegawa, Surf. Coat. Technol. 162 (2002) 1.
[10] W. Zhang, A. Tanaka, K. Wazumi, Y. Koga, B.S. Xu, Diamond Relat. Mater. 13 (2004) 2166.
[11] C.S. Lee, K.R. Lee, K.Y. Eun, K.H. Yoon, J.H. Han, Diamond. Relat. Mater. 11 (2002) 198.
[12] J.C. Damasceno, S.S. Camargo Jr., F.L. Freire Jr., R. Carius, Surf. Coat. Technol. 133–134 (2000) 247.
[13] M. Ikeyama, S. Nakao, Y. Miyagawa, S. Miyagawa, Surf. Coat. Technol. 191 (2005) 38.
[14] D.F. Franceschini, C.A. Achete, F.L. Freire Jr., Appl. Phys. Lett. 60 (1992) 3229.
[15] P. Papakonstantinou, J.F. Zhao, P. Lemoine, E.T. McAdams, J.A. McLaughlin, Diamond Relat. Mater. 11 (2002) 1074.
[16] M.G. Kim, K.R. Lee, K.Y. Eun, Surf. Coat. Technol. 112 (1999) 204.
[17] H. Hofsäss, H. Feldermann, R. Merk, M. Sebastian, C. Ronning, Appl. Phys. A 66 (1998) 153.
[18] J. Robertson, Diamond Relat. Mater. 2 (1993) 984.
[19] Y. Lifshitz, S.R. Kasi, J.W. Rabalais, Phys. Rev. Lett. 62 (1989) 1290.
[20] N.A. Marks, Diamond Relat. Mater. 14 (2005) 1223.
[21] B. Zheng, W.T. Zheng, S.S. Yu, H.W. Tian, F.L. Meng, Y.M. Wang, J.Q. Zhu, S.H. Meng, X.D. He, J.C. Han, Carbon 43 (2005) 1976.
[22] E. Neyts, A. Bogaerts, R. Gijbels, J. Benedikt, M.C.M. van de Sanden, Diamond Relat. Mater. 13 (2004) 1873.
[23] B.A. Pailthorpe, J. Appl. Phys. 70 (1991) 543.
[24] J. Tersoff, Phys. Rev. Lett. 56 (1986) 632.
[25] J. Tersoff, Phys. Rev. B 37 (1988) 6991.
[26] J. Tersoff, Phys. Rev. Lett. 61 (1988) 2879.
[27] J. Tersoff, Phys. Rev. B 39 (1989) 5566.
[28] N. Marks, J. Phys. Condens. Matter 14 (2002) 2901.
[29] S.H. Lee, C.S. Lee, S.C. Lee, K.H. Lee, K.R. Lee, Surf. Coat. Technol. 177–178 (2004) 812.
[30] H.U. Jäger, A.Yu. Belov, Phys. Rev. B 68 (2003) 024201(1).